THE JOURNAL OF PHYSICAL CHEMISTRY B

Article

pubs.acs.org/JPCB

Hyperpolarized *para*-Ethanol

Daniele Mammoli,*[,†] Basile Vuichoud,[†] Aurélien Bornet,[†] Jonas Milani,[†] Jean-Nicolas Dumez,[‡] Sami Jannin,[†,§] and Geoffrey Bodenhausen[†,∥,⊥,#]

[†]Institut des Sciences et Ingéniérie Chimiques, Ecole Polytechnique Fédérale de Lausanne, 1015 Lausanne, Switzerland

[‡]Institut de Chimie des Substances Naturelles (CNRS UPR 2301), 91190 Gif-sur-Yvette, France

[§]Bruker BioSpin AG, Industriestrasse 26, 8117 Fällanden, Switzerland

[∥]Département de Chimie, École Normale Supérieure-PSL Research University, 24 rue Lhomond, 75005 Paris, France

[⊥]Sorbonne Universités, UPMC Université Paris 06, LBM, 4 place Jussieu, 75005 Paris, France

[#]CNRS, UMR 7203 LBM, 75005 Paris, France

ABSTRACT: We show that an imbalance between the populations of singlet (S) and triplet (T) states in pairs of magnetically equivalent spins can be generated by dissolution dynamic nuclear polarization. In partly deuterated ethanol ($CD_3{}^{13}CH_2OD$), this T/S imbalance can be transferred by cross-relaxation to observable, enhanced signals of protons and coupled ^{13}C.

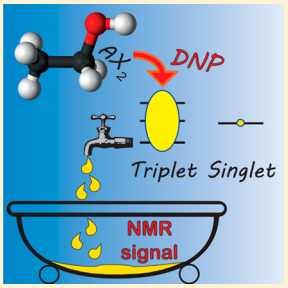

In recent years, long-lived states (LLSs)[1] and dynamic nuclear polarization (DNP)[2,3] have been extensively explored, since they offer novel means to overcome two major limitations of nuclear magnetic resonance (NMR), namely the short lifetime of nuclear magnetization (usually limited by the longitudinal relaxation time constant T_1) and the low intrinsic sensitivity of NMR and magnetic resonance imaging (MRI) that is normally governed by Boltzmann's law. LLS can preserve spin order over intervals much longer than T_1: this unique property is attractive for *in vivo* studies since it represents a promising way to use long-lived NMR signals of metabolites and characterize slow reactions that take place in tissues of interest.[4,5] Furthermore, dissolution-DNP (D-DNP)[6] is increasingly popular in metabolic in vivo studies and MRI since it enables *inter alia* the detection of anomalous metabolic behavior in tumors.[7−11] The combination of LLSs with DNP[12] and MRI[13] methods has recently been developed for applications on clinical MRI systems. The prototypical LLS is a "singlet state" of a pair of nuclear spins, which corresponds to a population imbalance[14] between the antisymmetric triplet manifold and the symmetric singlet state. In systems comprising two magnetically inequivalent spins, it is possible to populate LLSs directly by DNP at low spin temperatures.[15] LLSs can also be populated without resorting to DNP in systems with magnetically equivalent spins, as in the two-spin system of *para*-hydrogen[16] and in three-spin systems of methyl groups,[14,17−20] where manifolds of symmetry A and E correspond to irreducible representations of the C_3 group. In both cases, it is possible to induce a long-lived imbalance between states belonging to manifolds with different symmetries at moderately low temperature, provided the rotational energy gap is much larger than the Zeeman splitting. In *para*-hydrogen, the energy difference between the three triplet states and the singlet state S_0 is $\Delta E/k_B \sim 170$ K in the absence of a magnetic field, while in the methyl group of γ-picoline,[14] the difference between the A and E manifolds is only $\Delta E/k_B \sim 6$ K because of tunneling effects. In this Article, we show that, in an A_2 system with two magnetically equivalent spins, where the Zeeman energy difference between the triplet states T_{+1} and T_{-1} and the singlet state S_0 is $\Delta E/k_B \sim 14$ mK at $B_0 = 6.7$ T, it is possible to use D-DNP to induce a triplet−singlet imbalance (henceforth called TSI in analogy to the A/E imbalance, or AEI, in methyl groups[14]), which may be written as

$$\overline{|T\rangle\langle T|} - |S_0\rangle\langle S_0|$$

where $|S_0\rangle\langle S_0|$ is the population of the singlet state S_0 and $\overline{|T\rangle\langle T|}$ represents the mean population of the triplet manifold:

$$\overline{|T\rangle\langle T|} = 1/3[|T_{+1}\rangle\langle T_{+1}| + |T_0\rangle\langle T_0| + |T_{-1}\rangle\langle T_{-1}|]$$

Such an imbalance can be achieved by either enhancing or depleting the population of the singlet state with respect to the mean population of the triplet manifold. The major drawback of such a TSI is that it cannot be converted into observable magnetization unless the symmetry is broken, for example by a chemical reaction.[21,22] However, in an A_2X system where a spin X is coupled to the A_2 system, the TSI is slightly perturbed so

Received: December 5, 2014
Revised: January 28, 2015
Published: February 6, 2015

DOI: 10.1021/jp512128c
J. Phys. Chem. B 2015, 119, 4048−4052

that the magnetization can flow from the invisible *para*-state to observable population differences. The energy levels of the A_2X system can be derived from the singlet−triplet basis of the A_2 spins. Thus, if the third label designates the state of the X spin, we can define the following six triplet states:

$$T_{+1}^{\alpha} = |\alpha\alpha\alpha\rangle \qquad T_{+1}^{\beta} = |\alpha\alpha\beta\rangle$$

$$T_{0}^{\alpha} = \frac{|\alpha\beta\alpha\rangle + |\beta\alpha\alpha\rangle}{\sqrt{2}} \qquad T_{0}^{\beta} = \frac{|\alpha\beta\beta\rangle + |\beta\alpha\beta\rangle}{\sqrt{2}}$$

$$T_{-1}^{\alpha} = |\beta\beta\alpha\rangle \qquad T_{-1}^{\beta} = |\beta\beta\beta\rangle$$

and two singlet states:

$$S_{0}^{\alpha} = \frac{|\alpha\beta\alpha\rangle - |\beta\alpha\alpha\rangle}{\sqrt{2}} \qquad S_{0}^{\beta} = \frac{|\alpha\beta\beta\rangle - |\beta\alpha\beta\rangle}{\sqrt{2}}$$

In analogy with the A_2 case of two magnetically equivalent spins, we can consider the TSI or imbalance between the triplet and singlet manifolds:

$$\overline{|T\rangle\langle T|} - \overline{|S\rangle\langle S|}$$

where

$$\overline{|T\rangle\langle T|} = 1/3[|T_{+1}^{\alpha}\rangle\langle T_{+1}^{\alpha}| + |T_{0}^{\alpha}\rangle\langle T_{0}^{\alpha}| + |T_{-1}^{\alpha}\rangle\langle T_{-1}^{\alpha}| + |T_{+1}^{\beta}\rangle\langle T_{+1}^{\beta}| + |T_{0}^{\beta}\rangle\langle T_{0}^{\beta}| + |T_{-1}^{\beta}\rangle\langle T_{-1}^{\beta}|]$$

and

$$\overline{|S\rangle\langle S|} = [|S_{0}^{\alpha}\rangle\langle S_{0}^{\alpha}| + |S_{0}^{\beta}\rangle\langle S_{0}^{\beta}|]$$

The TSI corresponds to a difference of products of tensor operators T_{lp} of rank $l = 0$ and coherence order $p = 0$. Our experimental strategy to detect the TSI in an A_2X system comprises three steps: (i) *preparation* of a TSI through low temperature DNP at $T = 1.2$ K and $B_0 = 6.7$ T; (ii) *dissolution* of the sample by rapid heating to room temperature and transfer to an NMR (or MRI) system; (iii) *detection* of the stored TSI after transfer to observable population differences across the transitions of either ^{1}H or ^{13}C spins. This transfer is driven by cross-relaxation.

Preparation: A large TSI is obtained by dynamic nuclear polarization of ^{1}H spins at $T = 1.2$ K. Our sample consists of a mixture of 90% CD_3CH_2OD and 10% D_2O with 50 mM TEMPOL as polarizing agent. The solution forms a homogeneous glass upon freezing. Saturation of the electron spin resonance (ESR) transitions by monochromatic microwave irradiation at $f_{\mu w} = 188.3$ GHz induces an intense negative DNP effect. The steady-state proton polarization is $P(^1H) = -60\%$ (corresponding to a spin temperature of about −10 mK), and the build-up time constant is $\tau_{DNP}(^1H) = 122$ s, so that most spins are in the highest energy states $|\beta\beta\alpha\rangle$ and $|\beta\beta\beta\rangle$ that belong to the triplet manifold, while the singlet manifold is largely depleted, so that the resulting TSI reaches 12%.[15] Note that the two ^{1}H nuclei are not magnetically equivalent in the solid state because of their chemical shift anisotropy and intermolecular dipole−dipole couplings, so that transitions between the T and S manifolds are not forbidden. The sign of the TSI does not depend on the microwave frequency, provided that the energy of S_0 lies between the energies of T_{+1} and T_{-1} in an A_2 system, and a positive polarization populates the lowest state T_{+1} while depleting all other states. On the other hand, a negative polarization enhances the population of the highest state T_{-1}, with respect to all other states. Since positive or negative polarizations with equal magnitudes lead to the same mean population of the three triplet states, the TSI has the same sign regardless of the sign of the polarization.

Dissolution: After preparation of an imbalance between the triplet and singlet manifolds at low temperature, the DNP sample is rapidly dissolved with 5 mL degassed D_2O (preheated to $T = 450$ K at $p = 1.0$ MPa) in 0.7 s. The sample is then rapidly transferred with helium gas ($p = 0.6$ MPa) in 4.5 s to an NMR spectrometer through a home-built magnetic path[23] ($B > 0.9$ T). During this transfer the TSI is largely preserved.

Detection: To retain only the TSI and suppress any tensor operators T_{lp} of rank $l \neq 0$ and coherence order $p \neq 0$ that may have survived after the transfer, in particular in-phase magnetization T_{lp} with $l = 1$ and $p = 0$, suitable filters[24] are applied to ^{1}H and ^{13}C before the NMR signals are excited (Figure 1).

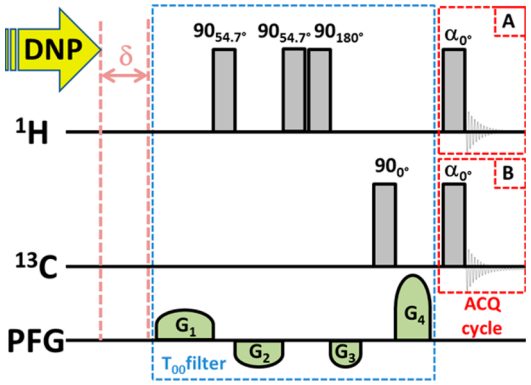

Figure 1. After D-DNP, a delay $\delta = 3$ s allows turbulences to settle. A T_{00} filter[24] is then applied to both protons and ^{13}C nuclei to suppress all first- and second-rank population distributions, thus retaining only terms of rank $l = 0$ associated with the T/S imbalance (TSI). The filter is followed by the acquisition of either ^{1}H (case A) or ^{13}C (case B) signals at intervals of 2.5 s.

After injection, proton signals can be excited by 5° pulses. The ^{13}C satellite peaks of the protons (^{13}C in 1.1% natural abundance) in the methylene group of $CD_3{}^{13}CH_2OD$ show an antiphase doublet due to $^1J(^1H, ^{13}C) = 143$ Hz (Figure 2A).

The ^{13}C spectra of the same isotopologue have been recorded by using either 9° pulses (Figure 2B) or 90° pulses (Figure 2C). In both cases, one observes ^{13}C multiplets that do not obey the usual binomial 1:2:1 intensity distribution of $^{13}CH_2$ groups. The proton and carbon-13 signals arise because cross-relaxation converts the invisible TSI into observable population differences across allowed transitions. The non-binomial peak patterns have the same sign regardless if one saturates either the positive or negative lobes of the microwave DNP response. The enhancements ε are determined by comparison to Boltzmann's polarization in thermal equilibrium, as reported in Table 1.

Simulations were carried out using the Mathematica package *SpinDynamica*.[25] The initial state consisted of a pure TSI, and the relaxation superoperator accounted for dipole−dipole (DD) interactions, the chemical shift anisotropies (CSAs) of both ^{1}H and ^{13}C, and DD/CSA cross-correlation effects. For simplicity, the proton CSA tensors were assumed to have only two distinct principal axes, with their unique axis parallel to the C−H bonds. Inspired by an elegant work of Brown, Price, and

DOI: 10.1021/jp512128c
J. Phys. Chem. B 2015, 119, 4048−4052

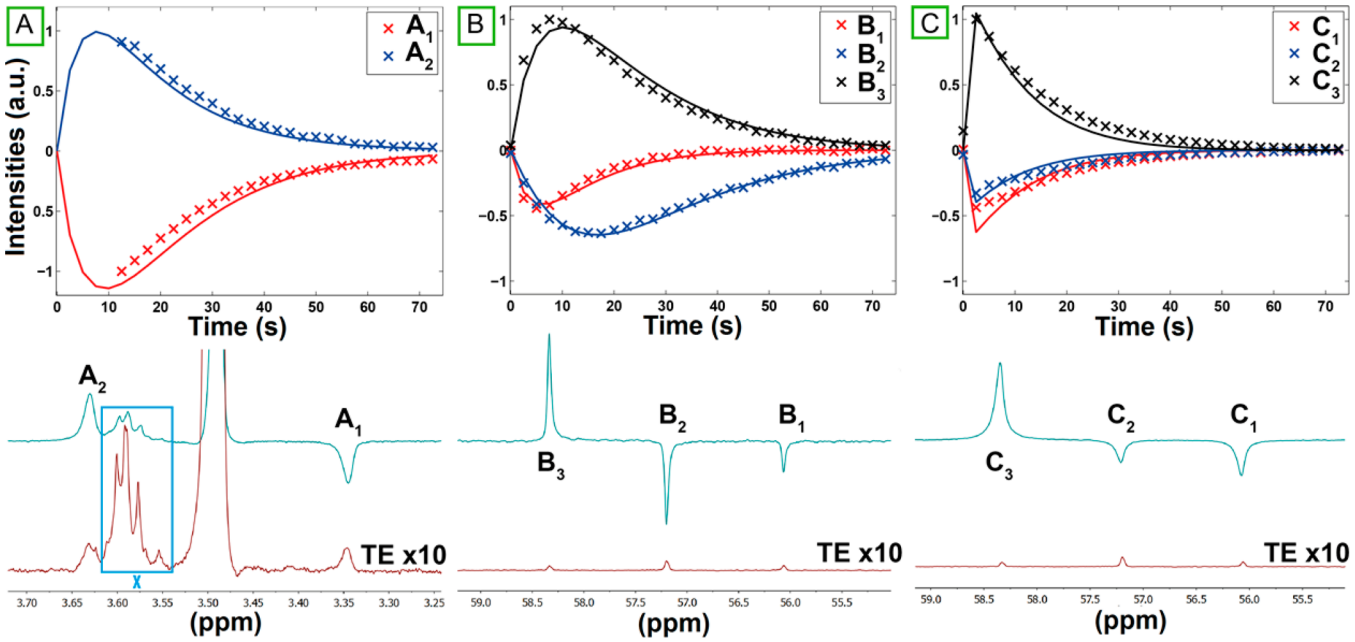

Figure 2. [Top] Experimental (crosses) and simulated (lines) time-dependence of hyperpolarized ^{1}H and ^{13}C signals of the $^{13}CH_2$ group in $CD_3{}^{13}CH_2OD$ with ^{13}C in natural 1.1% abundance, recorded every 2.5 s, starting 5 s after injection following the transfer from the DNP polarizer, at ambient temperature in a field B_0 = 11.66 T (500 MHz for protons), using the sequence in Figure 1. (A) Intensities of the ^{13}C satellite peaks in the ^{1}H spectra observed with 5° pulses. (B) Intensities of the three ^{13}C triplet components observed with 9° pulses. (C) The same as B but observed with 90° pulses. The solid lines have been simulated by *SpinDynamica*[25] (see text for details). [Bottom] Enhanced spectra (green) observed at the highest amplitudes of the time-dependent signals shown above, for comparison with thermal equilibrium (TE) spectra amplified by a factor 10 (red). The enhancement factors are shown in Table 1. Experiments and simulations were scaled independently in each panel. The first points in A have been discarded due to baseline distortions. The signals marked X are due to impurities.

Table 1. Relaxation Times T_1 and T_{decay} and Enhancement Factors ε for Different Peaks (Labeled as in Figure 2)

	^{13}C satellite peaks in ^{1}H spectra		$^{13}CH_2$ triplet components in ^{13}C spectra					
	A_1	A_2	B_1	B_2	B_3	C_1	C_2	C_3
T_1 determined by inversion recovery (s)	8.6 ± 0.6	7 ± 2	9 ± 1	12 ± 1	10 ± 1	9 ± 1	12 ± 1	10 ± 1
T_{decay} determined from time-dependence (s)	17.7 ± 0.5	17.8 ± 0.6	10 ± 1	17 ± 2	18 ± 1	17.5 ± 0.7	17.6 ± 0.5	14.8 ± 0.4
enhancement ε	~20	~20	~150	~100	~310	~160	~60	~350

The T_1 values were determined by inversion recovery experiments. The time constants T_{decay} were determined by fitting the time-dependence in Figure 2A,B to biexponential functions $k_1{\cdot}\exp(-t/T_{build\text{-}up}) + k_2{\cdot}\exp(-t/T_{decay})$ and in Figure 2C to monoexponential function $k{\cdot}\exp(-t/T_{decay})$. The enhancements ε are defined as the ratio of the peaks at the maximum amplitude of the time-dependent signals and the spectra in thermal equilibrium, obtained with the same flip angle.

Grant,[26] rotational diffusion was modeled by a symmetric top with a fast diffusion axis perpendicular to the CH_2 plane and two slow diffusion axes lying in that plane. The diffusion constants $D_{fast} = 1.7 \times 10^{11}$ s^{-1} and $D_{slow} = 1.5 \times 10^{10}$ s^{-1} and the CSA parameters $\Delta\sigma^{1H} = 7$ ppm and $\Delta\sigma^{13C} = 66$ ppm were adjusted to obtain a reasonable agreement between the experimental and simulated time-dependence. The predicted enhancements are larger than those observed experimentally; the discrepancy may be explained by losses during the transfer step. The agreement shown in Figure 2 speaks in favor of the proposed mechanism where the TSI generated by DNP is spontaneously converted by cross-relaxation into population differences across observable transitions.

The longitudinal relaxation times have been determined by inversion recovery experiments. $T_1(^1H)$ refers to the two ^{13}C satellite peaks in the proton spectra, while $T_1(^{13}C)$ refers to the three components of the nonbinomial ^{13}C triplet. The time-dependence in Figure 2A,B has been fitted to biexponential functions:

$$k_1{\cdot}\exp(-t/T_{build-up}) + k_2{\cdot}\exp(-t/T_{decay})$$

describing the build-up and decay of the signals, the first time constant being smaller than but close to the experimental T_1. In Figure 2C, a monoexponential function

$$k{\cdot}\exp(-t/T_{decay})$$

was used. Enhancements in Table 1 correspond to the ratios of the maximum amplitudes of the time-dependent signals and the spectra obtained in thermal equilibrium at room temperature using the same flip angles. The time constants T_{decay} are somewhat longer than $T_1(^1H)$ and $T_1(^{13}C)$, with averaged ratios $T_{decay}/T_1(^1H) \sim 2.3$ and $T_{decay}/T_1(^{13}C) \sim 1.5$, suggesting a moderately long-lived behavior of both proton and carbon-13 polarizations. These ratios are not very favorable, but longer-lived states might be found in systems where the spy nucleus is more remote and, therefore, less strongly coupled to the two nuclei carrying the LLS. Geometrical optimization could be helpful to boost these lifetimes.[27−29]

DOI: 10.1021/jp512128c
J. Phys. Chem. B 2015, 119, 4048−4052

In conclusion, we have shown that dissolution dynamic nuclear polarization can be used to generate a T/S imbalance (or TSI) between the triplet and singlet manifolds in a system comprising two magnetically equivalent proton spins. If the two protons are coupled to a "spy" ^{13}C spin, this imbalance gives rise to substantially enhanced proton and carbon NMR spectra by spontaneous cross-relaxation of the TSI into population differences across observable transitions. This leads to characteristic nonbinomial ^{1}H and ^{13}C multiplets of the methylene group of partially deuterated ethanol $CD_3{}^{13}CH_2OD$ with ^{13}C in natural isotopic abundance. Our experimental scheme to detect a TSI though a coupled spin should be widely applicable in any molecule containing a $^{13}CH_2$ group.

AUTHOR INFORMATION

Corresponding Author

*E-mail: daniele.mammoli@epfl.ch.

Author Contributions

All authors have contributed to the manuscript; all have given approval to the final version of the manuscript.

Notes

The authors declare no competing financial interest.

ACKNOWLEDGMENTS

Funding for this work was provided by the Swiss National Science Foundation (SNSF), the Swiss "Commission pour la Technologie et l'Innovation" (CTI), the "École polytechnique fédérale de Lausanne" (EPFL), the French "Centre national de la recherche scientifique" (CNRS), and the "European Research Council" (ERC, grant "dilute *para*-water"). We are indebted to Malcom H. Levitt and Giuseppe Pileio for stimulating discussions.

ABBREVIATIONS

TSI, triplet-singlet imbalance; D-DNP, dissolution dynamic nuclear polarization; LLS, long-lived state; NMR, nuclear magnetic resonance; DD, dipole−dipole; CSA, chemical shift anisotropy

REFERENCES

(1) Carravetta, M.; Johannessen, O. G.; Levitt, M. H. Beyond the T-1 Limit: Singlet Nuclear Spin States in Low Magnetic Fields. *Phys. Rev. Lett.* **2004**, *92*, 153003.

(2) Carver, T.; Slichter, C. Polarization of Nuclear Spins in Metals. *Phys. Rev.* **1953**, *92*, 212−213.

(3) Carver, T.; Slichter, C. Experimental Verification of the Overhauser Nuclear Polarization Effect. *Phys. Rev.* **1956**, *102*, 975−980.

(4) Pileio, G.; Carravetta, M.; Levitt, M. H. Storage of Nuclear Magnetization as Long-Lived Singlet Order in Low Magnetic Field. *Proc. Natl. Acad. Sci. U. S. A.* **2010**, *107*, 17135−17139.

(5) Marco-Rius, I.; Tayler, M. C. D.; Kettunen, M. I.; Larkin, T. J.; Timm, K. N.; Serrao, E. M.; Rodrigues, T. B.; Pileio, G.; Ardenkjaer-Larsen, J. H.; Levitt, M. H.; et al. Hyperpolarized Singlet Lifetimes of Pyruvate in Human Blood and in the Mouse. *NMR Biomed.* **2013**, *26*, 1696−1704.

(6) Ardenkjaer-Larsen, J. H.; Fridlund, B.; Gram, A.; Hansson, G.; Hansson, L.; Lerche, M. H.; Servin, R.; Thaning, M.; Golman, K. Increase in Signal-to-Noise Ratio of > 10,000 Times in Liquid-State NMR. *Proc. Natl. Acad. Sci. U. S. A.* **2003**, *100*, 10158−10163.

(7) Park, I.; Larson, P. E. Z.; Zierhut, M. L.; Hu, S.; Bok, R.; Ozawa, T.; Kurhanewicz, J.; Vigneron, D. B.; VandenBerg, S. R.; James, C. D.; Nelson, S. J. Hyperpolarized ^{13}C Magnetic Resonance Metabolic Imaging: Application to Brain Tumors. *Neuro-Oncol.* **2010**, *12*, 133−144.

(8) Day, S. E.; Kettunen, M. I.; Gallagher, F. A.; Hu, D.-E.; Lerche, M.; Wolber, J.; Golman, K.; Ardenkjaer-Larsen, J. H.; Brindle, K. M. Detecting Tumor Response to Treatment Using Hyperpolarized C-13 Magnetic Resonance Imaging and Spectroscopy. *Nat. Med.* **2007**, *13*, 1382−1387.

(9) Brindle, K. New Approaches for Imaging Tumour Responses to Treatment. *Nat. Rev. Cancer* **2008**, *8*, 94−107.

(10) Gallagher, F. A.; Kettunen, M. I.; Hu, D.-E.; Jensen, P. R.; in't Zandt, R.; Karlsson, M.; Gisselsson, A.; Nelson, S. K.; Witney, T. H.; Bohndiek, S. E.; et al. Production of Hyperpolarized [1,4-C-13(2)]malate from [1,4-C-13(2)]fumarate Is a Marker of Cell Necrosis and Treatment Response in Tumors. *Proc. Natl. Acad. Sci. U. S. A.* **2009**, *106*, 19801−19806.

(11) Albers, M. J.; Bok, R.; Chen, A. P.; Cunningham, C. H.; Zierhut, M. L.; Zhang, V. Y.; Kohler, S. J.; Tropp, J.; Hurd, R. E.; Yen, Y.-F.; Nelson, S. J.; Vigneron, D. B.; Kurhanewicz, J. Hyperpolarized ^{13}C Lactate, Pyruvate, and Alanine: Noninvasive Biomarkers for Prostate Cancer Detection and Grading. *Cancer Res.* **2008**, *68*, 8607−8615.

(12) Bornet, A.; Jannin, S.; Bodenhausen, G. Three-Field NMR to Preserve Hyperpolarized Proton Magnetization as Long-Lived States in Moderate Magnetic Fields. *Chem. Phys. Lett.* **2011**, *512*, 151−154.

(13) Pileio, G.; Bowen, S.; Laustsen, C.; Tayler, M. C. D.; Hill-Cousins, J. T.; Brown, L. J.; Brown, R. C. D.; Ardenkjaer-Larsen, J. H.; Levitt, M. H. Recycling and Imaging of Nuclear Singlet Hyperpolarization. *J. Am. Chem. Soc.* **2013**, *135*, 5084−5088.

(14) Meier, B.; Dumez, J.-N.; Stevanato, G.; Hill-Cousins, J. T.; Roy, S. S.; Hakansson, P.; Mamone, S.; Brown, R. C. D.; Pileio, G.; Levitt, M. H. Long-Lived Nuclear Spin States in Methyl Groups and Quantum-Rotor-Induced Polarization. *J. Am. Chem. Soc.* **2013**, *135*, 18746−18749.

(15) Tayler, M. C. D.; Marco-Rius, I.; Kettunen, M. I.; Brindle, K. M.; Levitt, M. H.; Pileio, G. Direct Enhancement of Nuclear Singlet Order by Dynamic Nuclear Polarization. *J. Am. Chem. Soc.* **2012**, *134*, 7668−7671.

(16) Bowers, C.; Weitekamp, D. Transformation of Symmetrization Order to Nuclear Spin Magnetization by Chemical Reaction and Nuclear Magnetic Resonance. *Phys. Rev. Lett.* **1986**, *57*, 2645−2648.

(17) Tomaselli, M.; Degen, C.; Meier, B. H. Haupt Magnetic Double Resonance. *J. Chem. Phys.* **2003**, *118*, 8559−8562.

(18) Tomaselli, M.; Meier, U.; Meier, B. H. Tunneling-Induced Spin Alignment at Low and Zero Field. *J. Chem. Phys.* **2004**, *120*, 4051−4054.

(19) Haupt, J. New Effect of Dynamic Polarization in a Solid Obtained by Rapid Change of Temperature. *Phys. Lett. A* **1972**, *A 38*, 389−&.

(20) Icker, M.; Fricke, P.; Berger, S. Transfer of the Haupt-Hyperpolarization to Neighbor Spins. *J. Magn. Reson.* **2012**, *223*, 148−150.

(21) Bornet, A.; Ji, X.; Mammoli, D.; Vuichoud, B.; Milani, J.; Bodenhausen, G.; Jannin, S. Long-Lived States of Magnetically Equivalent Spins Populated by Dissolution-DNP and Revealed by Enzymatic Reactions. *Chem.—Eur. J.* **2014**, *20*, 17113−17118.

(22) Warren, W. S.; Jenista, E.; Branca, R. T.; Chen, X. Increasing Hyperpolarized Spin Lifetimes Through True Singlet Eigenstates. *Science* **2009**, *323*, 1711−1714.

(23) Milani J.; Vuichoud B.; Bornet A.; Miéville P.; Mottier R.; Jannin S.; Bodenhausen G. A Magnetic Path to Shelter Hyperpolarized Fluids. *Rev. Sci. Instrum.*, DOI: 10.1063/1.4908196.

(24) Tayler, M. C. D.; Levitt, M. H. Accessing Long-Lived Nuclear Spin Order by Isotope-Induced Symmetry Breaking. *J. Am. Chem. Soc.* **2013**, *135*, 2120−2123.

(25) Levitt M. H. et al. SpinDynamica, available at www.spindynamica.soton.ac.uk.

(26) Brown, R. A.; Price, R. H.; Grant, D. M. Detecting Proton Magnetization via 13C-Coupled Relaxation Studies. *J. Magn. Reson. A* **1994**, *110*, 38−44.

DOI: 10.1021/jp512128c
J. Phys. Chem. B 2015, 119, 4048−4052

(27) Ahuja, P.; Sarkar, R.; Vasos, P. R.; Bodenhausen, G. Molecular Properties Determined from the Relaxation of Long-Lived Spin States. *J. Chem. Phys.* **2007**, *127*, 134112.
(28) Grant, A. K.; Vinogradov, E. Long-Lived States in Solution NMR: Theoretical Examples in Three- and Four-Spin Systems. *J. Magn. Reson.* **2008**, *193*, 177−190.
(29) Pileio, G. Singlet State Relaxation via Intermolecular Dipolar Coupling. *J. Chem. Phys.* **2011**, *134*, 214505.

DOI: 10.1021/jp512128c
J. Phys. Chem. B 2015, 119, 4048−4052